

# Analyst

Accepted Manuscript



This is an *Accepted Manuscript*, which has been through the Royal Society of Chemistry peer review process and has been accepted for publication.

*Accepted Manuscripts* are published online shortly after acceptance, before technical editing, formatting and proof reading. Using this free service, authors can make their results available to the community, in citable form, before we publish the edited article. We will replace this *Accepted Manuscript* with the edited and formatted *Advance Article* as soon as it is available.

You can find more information about *Accepted Manuscripts* in the [Information for Authors](#).

Please note that technical editing may introduce minor changes to the text and/or graphics, which may alter content. The journal's standard [Terms & Conditions](#) and the [Ethical guidelines](#) still apply. In no event shall the Royal Society of Chemistry be held responsible for any errors or omissions in this *Accepted Manuscript* or any consequences arising from the use of any information it contains.

# Rapid, Highly Sensitive Detection of Herpes Simplex Virus-1 using Multiple Antigenic Peptide-Coated Superparamagnetic Beads

Ying-Fen Ran<sup>a,b</sup>, Conor Fields<sup>a,b</sup>, Julien Muzard<sup>a</sup>, Viktoriya Liauchuk<sup>a</sup>, Michael Carr<sup>c</sup>, William Hall<sup>c</sup>, and Gil U Lee<sup>a\*</sup>

<sup>5</sup> Received (in XXX, XXX) Xth XXXXXXXXXX 20XX, Accepted Xth XXXXXXXXXX 20XX

DOI: 10.1039/b000000x

A sensitive, rapid, and label free magnetic bead aggregation (MBA) assay has been developed that employs superparamagnetic (SPM) beads to capture, purify, and detect model proteins and the herpes simplex virus (HSV). The MBA assay is based on monitoring the aggregation state of a population of SPM beads using light scattering of individual aggregates. A biotin-streptavidin MBA assay had a femtomolar (fM) level sensitivity for analysis times less than 10 minutes, but the response of the assay becomes nonlinear at high analyte concentrations. A MBA assay for the detection of HSV-1 based on a novel peptide probe resulted in the selective detection of the virus at concentrations as low as 200 viral particles (vp) per mL in less than 30 min. We define the parameters that determine the sensitivity and response of the MBA assay, and the mechanism of enhanced sensitivity of the assay for HSV. The speed, relatively low cost, and ease of application of the MBA assay promise to make it useful for the identification of viral load in resource-limited and point-of-care settings where molecular diagnostics cannot be easily implemented.

## Introduction

HSV-1 and 2 are large (>150 kb), double-stranded DNA viruses from the Herpesviridae family that are transmitted to humans by direct skin-to-skin contact, in the case of HSV-1 by contact with the orofacial region, and for HSV-2 through sexual routes. Between 60%-95% of adults worldwide are infected by herpes simplex virus.<sup>1</sup> Symptoms include sores or blisters around the infected region, causing discomfort and in some cases, pain, for the individual. Although rare, HSV infection of the central nervous system can occur, resulting in herpes simplex encephalitis (HSE), which is fatal in 70% of untreated cases.<sup>2</sup> The clinical outcome of HSV infection can be favourable if antiviral therapy is appointed in the early stages of infection, accentuating the need for rapid diagnostic assays.

The gold standard HSV diagnostic test involves the monitoring of cytopathic effects of the virus on susceptible cell cultures. While highly sensitive and specific, results can take up to one week to complete.<sup>3</sup> To circumvent time issues, polymerase chain reaction (PCR), has been proposed as an alternative diagnostic assay, which maintains high sensitivity and specificity, but requires trained personnel and remains time consuming (4h).<sup>4</sup> Other diagnostic procedures such as enzyme immunoassay (EIA) and fluorescent antibody tests (FAT) typically take several hours to conduct and suffer from poor sensitivity.<sup>5,6</sup> As a result, these tests are rarely used as the sole means of detection. To improve therapy uptake, new assays are needed to enable rapid diagnosis in a point of care (POC) setting.

Bioanalytical testing often requires a pretreatment stage involving filtration and/or purification. SPM beads, composed of

assemblies of iron oxide nanoparticles, provide a rapid, efficient, and cost effective way to pre-concentrate or separate an analyte from complex materials to simplify and facilitate the front-end of an assay. They are readily available through a number of synthetic strategies and commercial sources,<sup>7</sup> offering a range of chemistries suitable for separation. SPMs have demonstrated their versatility for use in conjunction with techniques such as the polymerase chain reaction<sup>8</sup> and mass spectroscopy,<sup>9</sup> and have been utilized in high-throughput linear magnetophoresis (LM) assays.<sup>10-14</sup> Importantly, if the analyte contains multiple epitopes, it is possible for the target to bind to multiple beads simultaneously, leading to bead aggregation.<sup>10, 15-17</sup> Exploiting aggregation as an analytical signal allows for a simple, label-free detection strategy. This process has been utilized in LM, allowing the detection of dengue virus as low as 10 plaque forming units/mL.<sup>10</sup>

Central to any affinity-based detection is the choice of probe. Structurally, herpes simplex virus is highly complex, and comprises three major structural elements, namely, the inner nucleo-capsid, the tegument, and the envelope on the exterior. The envelope has been shown to contain up to 750 glycoprotein spikes, varying in length, spacing and their protruding angles.<sup>18</sup> This complexity makes the generation of affinity ligands targeting HSV challenging. While antibodies remain the gold standard in immunodiagnostics, the viability of peptide-based viral diagnostic assays is being increasingly recognized.<sup>19-21</sup> Identification of peptide ligands by phage display technology, and subsequent production by solid phase peptide synthesis (SPPS), offers an elegant and inexpensive alternative to the generation of antibody ligands, while maintaining affinity and

specificity similar to naturally occurring protein-based ligands. Moreover, the synthetic nature of peptide ligands affords the option to improve and optimize interaction with the target through sequence variation.<sup>22</sup> Interestingly, reports suggest that the generation of multiple antigenic peptides (MAPs) enhances binding of monovalent peptide counterparts,<sup>23-25</sup> due to the creation of an observed avidity effect when multiple binding events occur. In this article we describe the screening of a linear dodecameric peptide phage display library to identify novel peptide-based ligands for high affinity binding of HSV-1.

**Figure 1** illustrates the principle of the MBA assay. The virus was first incubated with the peptide functionalized SPM beads, depicted in **Figure 1B**, and in the second step a magnetic gradient was applied to the bead suspension, to separate the beads and accelerate the rate of bead interaction. The ability to monitor changes in size, as well as fluorescence, of individual bead aggregates makes flow cytometry (FC) an attractive technology platform for MBA assays. The magnetic separation procedure is rapid, and requires as little as 2 min with FC analysis producing sample sizes as high as 100,000 particles in 5 minutes. In this article we describe the development and performance of MBA assays for a model biotin-streptavidin and subsequently HSV-1, defining sensitivity, response time, and the nonlinear response of the assay at high concentrations of analyte.

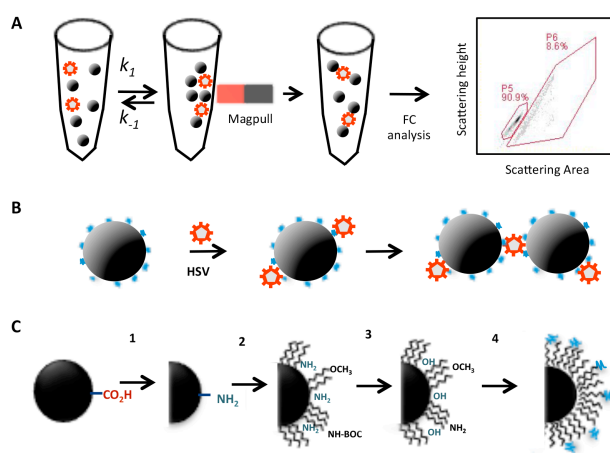


**Figure 1.** MBA assay for HSV-1 based on single particle light scattering. **A.** Anti-HSV-1 SPM beads were incubated with HSV-1 and the aggregation of the beads was aided by the application of a magnetic field. The final aggregation state of the beads was determined using FC. **B.** Schematic of the capture of HSV-1 using peptide functionalized SPM beads and assembly of SPM bead aggregates as a result of magnetic aggregation. **C.** Chemistry used to modify the SPM beads with affinity ligands. (1) Carboxyl beads were modified with a PEI monolayer, (2) a mixed BOC and methoxy-PEG monolayer was grafted onto this amine-derivatized surface, (3) the BOC-PEGs were deprotected, and (4) the thiolated MAP was coupled to maleimide-activated NH<sub>2</sub>-PEGs.

## Experimental Section

### Peptide design, synthesis and characterization

The preparation of the bacteriophage library and screening has been described in the *Supporting Information*. Peptide selection was based on phage ELISA assays of clones selected against HSV-1 as described in the *Supporting Information*. The three identified linear dodecapeptides, i.e., **N** - NHVHRMHATPAY, **E** - EHMALTYFRPP and, **G** - GPKALSPLMRMG, were synthesized at >95 % purity (Entelechon, Germany). The C-terminus of these peptides was elongated with a GGGs-CONH<sub>2</sub> moiety to mimic the GGGs-peptide spacer between the random peptide sequence tethered to the bacteriophage pIII protein and to block the negative charge of the carboxyl terminus. The ability of biotinylated synthetic peptides to bind purified HSV-1 was analyzed using a solid phase assay. In this case, 10 µg/mL of peptide in PBS buffer was incubated on HSV-coated wells (100 g/mL) and detected using a streptavidin-HRP conjugate. Binding and absorbance readings were carried out using the TMB substrate as described previously.<sup>32</sup> For the aggregation assays, biotinylated and cysteine-terminated peptides, based on the best peptide candidate, were generated in a multimeric, branched format, i.e., (GPKALSPLMRMG)<sub>4</sub>-K<sub>2</sub>KGGS-K(Biotin) and (GPKALSPLMRMG)<sub>4</sub>K<sub>2</sub>KGSGCG).

### Preparation of peptide and antibody functionalized SPMs

Three types of SPM beads were used in this study, i.e., streptavidin, antibody, or peptide functionalized beads. Anti-HSV functionalized beads were created by coupling the antibody to protein A functionalized beads. This was achieved by reacting the anti-HSV-1 antibody at 0.1 mg/mL with the protein A beads (3 mg) in 800 µL PBS buffer for 1 hr on a rotating wheel at room temperature. After incubation, antibody coated beads were washed with PBST buffer and stored with PBST with 0.1 (wt/wt%) BSA at 4 °C. The peptide functionalized beads were prepared either through self-assembly of biotinylated peptides on streptavidin SPM beads or covalent immobilization of thiol functionalized peptides on PEG SPM beads. The three biotinylated, multimeric peptide beads, i.e., MAP-G, MAP-N and MAP-E, were prepared by incubating the biotinylated multimeric peptides at 2 mg/mL with streptavidin beads (3mg) in 1mL PBS buffer for 1 hour. After three washes with PBST (0.1%), the three different peptide-functionalized beads were stored until further use with 0.1 (wt/wt%) BSA at 4°C. Two variations of the peptide beads were generated by covalently coupling the peptides to PEG functionalized beads, i.e., SPM-G2 and SPM-G3, using the four-step surface chemistry presented in **Figure 1C**. The carboxyl SPM beads were first functionalized with a primary amine monolayer using a two-step chemistry, i.e., 1 ml of carboxyl coated beads (5 mg/mL) were activated with a solution of 5 mg EDC and 5 mg sulfo-NHS in 0.5 ml MES buffer; and these beads were reacted with a 1 ml solution of 5% PEI in carbonate buffer. The beads were then modified with a monolayer of PEG, i.e., a mixture of hetrobifunctional PEGs (10 mg/mL) in 0.6 M K<sub>2</sub>SO<sub>4</sub> was added to 1 ml of the amine modified beads and reacted for 2 h at 50°C. The ratio of BOC-NH-PEG-NHS and methoxy-PEG-NHS used was either 1:3 for the SPM-G2 beads or 1:0 for the SPM-G3 beads. The unreacted primary and secondary amines on the beads were then capped using a two-step procedure, i.e., the beads were activated with 1 mg/ml of SMCC in a solution of 25% DMSO and 75% PBST for 1 hr, and the maleimide group was then capped by reacting the beads with 5% (V/V)

mercaptoethanol in PBS 2 hrs. The deprotection of the primary amine was achieved by reacting the beads with 60% (v/v) trifluoroacetic acid (TFA) in PBST buffer. MAP-G with a terminal cysteine was then coupled to the beads using the sulfosuccinimidyl 4-[N-maleimidomethyl]cyclohexane-1-carboxylate (SMCC) coupling chemistry. Each stage of the reaction was characterized with zeta potential measurements, as shown in Figure S4.

### Magnetic Bead Aggregation (MBA) Assay

Figures 1A and B illustrate the steps of the MBA assay and FC analysis. Samples of HSV or BBSA were prepared by dilution at the required concentration in a 300  $\mu$ L volume of PBST. SPM bead aliquots were added to the solution containing the target, and the concentration of beads was set to  $2 \times 10^6$  beads/mL in the final dilution. The solution was incubated at room temperature on a rotating wheel for 30 min for HSV and 2, 5 and 30 min for BBSA. After the required reaction time, the sample was subjected to magnetic field assisted aggregation, i.e., the sample containing SPMs was placed next to a NdBFe magnet with a field strength of 2.5 kGauss until the majority of the beads came out of solution. Once the SPMs were collected the tube was rotated 90 degrees in the magnetic field. This allowed the SPM beads to roll over each other on the side of the container.

### Flow cytometry

Particle aggregation measurements were performed using a flow cytometer with blue and red lasers, two light scattering detectors, and four fluorescence detectors with optical filters. The assay sample was placed into the flow cytometer instrument and the sample was analyzed until 10,000 events had been recorded (threshold in 80,000). As shown in Figure S1 (Supporting Information) the number of monomers and aggregates in the sample were determined by gating individual areas of the scatter plots with the forward scattering area (FSC-A) against forward scattering height (FSC-H). Individual monomers have lower FSC-A and FSC-H values, and thus are confined to a narrow area in the bottom-left hand corner of the plots. Conversely, aggregated beads are easily identified and discriminated from monomers due to the higher FSC-A and FSC-H values. Each assay was run in triplicate and the average values are plotted in all graphs.

## Results and Discussion

### Detection of biotinylated bovine serum albumin (BBSA) using streptavidin functionalized SPMs

The principle of MBA-FC assay was initially investigated using the model streptavidin-biotin molecular recognition system. Biotinylated bovine serum albumin (BBSA), where each BSA protein was functionalized with an average of 9 biotin molecules, was detected with highly uniform  $2.8 \mu$ m streptavidin functionalized SPMs. Figure 2 presents the FC analysis of the BBSA-streptavidin MBA assay performed at a bead concentration of  $2.0 \times 10^6$  beads/mL at three different reaction times of 2, 5 and 30 min. The scattering of a population of  $2 \times 10^5$  particles, shown in Figure 2A, fell into distinct sub-populations in which the intensity of scattering was proportional to the area of scattering (as measured by FC). This allowed us to identify the

number density of monomers as well as dimeric, trimeric, and tetrameric aggregates, which scattered light more intensely. The use of the same number of beads for each measurement ensured that the formation of aggregates was directly related to the observed decrease in monomers, i.e., the maximum number of aggregates was observed (Figure 2B) at the BBSA concentration with the minimum number of monomers (Figure 2C). The density of aggregates was observed to increase as the concentration of BBSA increased from  $3 \times 10^{-15}$  to  $3 \times 10^{-9}$  M, as shown in Figure 2B. Increasing the reaction time from 2 to 30 min did not produce a significant variation in the density of aggregates ( $p < 0.02$ ) except at concentrations of  $3 \times 10^{-15}$  and  $3 \times 10^{-13}$  M. At concentrations of BBSA greater than 1 nM there was a sharp decrease in the number of aggregates and an increase in monomers for all reaction times. The decrease in the aggregate signal at high concentrations of BBSA resulted from the saturation of the streptavidin on the beads, which we will refer to as the 'hook' effect. It was also observed that a significant number of larger aggregates were formed at  $10^{-9}$  M BBSA concentrations, which was characteristic of the higher coverage of biotin on the beads.

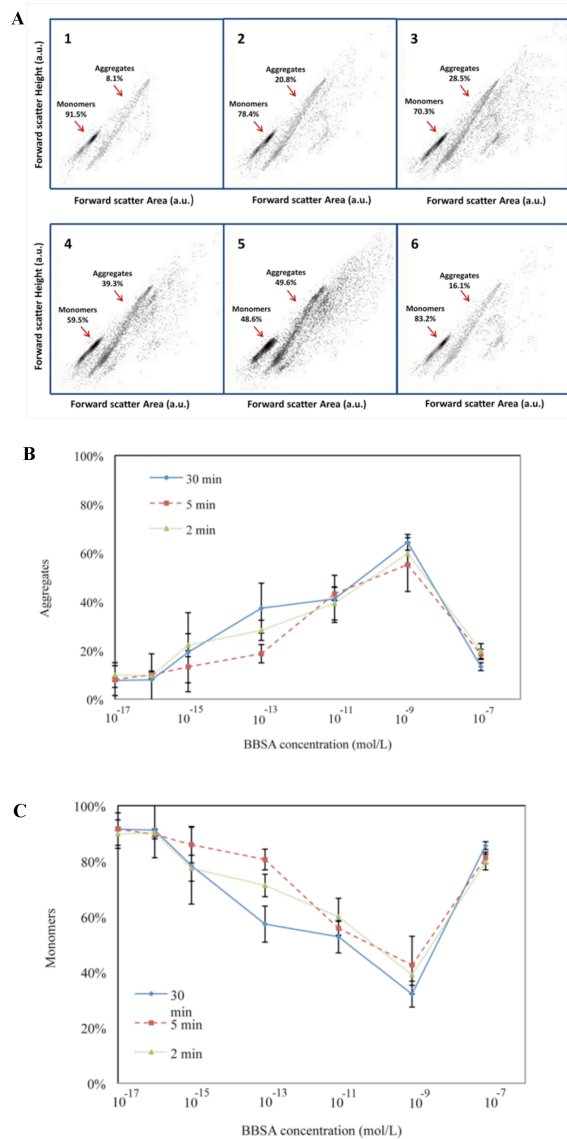


**Figure 2.** Results of the MBA assay for the detection of BBSA. **A.** Flow cytometry analysis of BBSA-streptavidin bead assays: (1) blank and (2) BBSA in the concentration of  $3 \times 10^{-15}$ , (3)  $3 \times 10^{-13}$ , (4)  $3 \times 10^{-11}$ , (5)  $3 \times 10^{-9}$ , and (6)  $3 \times 10^{-7}$  M. **B** Proportion of aggregates and **C** monomers formed as a function BBSA concentration. The incubation of the BBSA with the SPM beads was conducted for 2, 5 and 30 min reaction times, and three measurements were made at each BBSA concentration.

### B. Influence of reaction and mass transfer rates on the MBA assay

**Figure 3** illustrates the influence that the binding capacity and number of SPM beads have on the sensitivity of the MBA assay and onset of the hook effect (results are presented in the *Supplementary Information* section). In this section we examine the role that chemical and physical factors play in the response of the BBSA MBA assay.

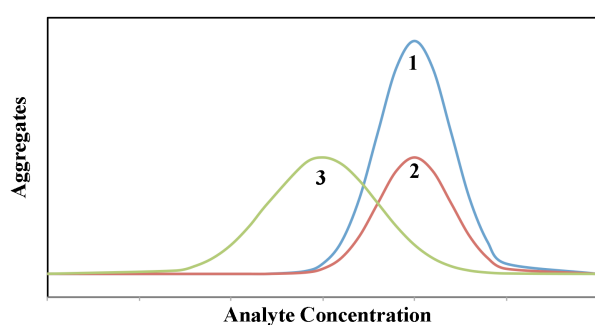
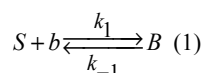


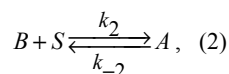
**Figure 3.** MBA assay response resulting from the change in physical and chemical properties of the SPM beads. (1) Reference binding curve, (2) decrease in ligand density on the beads, and (3) decrease in the number of beads used in the assay.

The formation of aggregates of beads in the MBA assay was the result of two reactions. In the first step BBSA ( $b$ ) reacted with the streptavidin on the beads ( $S$ ) to produce a biotinylated bead ( $B$ )



where  $k_1$  and  $k_{-1}$  are the forward and reverse rates of reaction, respectively. The rate constants of this reaction resulted from the convective mass transport of the BBSA to the surface of the beads ( $h$ ) and the reaction of the BBSA with the streptavidin immobilized on the beads ( $k_{S,b}$ ). The relative importance of these two parameters on the overall rate of reaction is characterized by the second Damkohler number ( $Da_{II}$ ), and the fact that  $Da_{II}$  was less than one over the range of streptavidin concentrations used in this study indicated that the rate constant was dominated by  $k_{S,b}$  (results presented in the *Supplementary Information* section).

The second MBA reaction involves the interaction of BBSA on one bead ( $B$ ) with the streptavidin on another bead ( $S$ ) resulting in the formation of bead aggregates ( $A$ )



where  $k_2$  and  $k_{-2}$  are the forward and reverse reaction rates of the

beads, respectively. The rate constants of this reaction are determined by the rate of encounter of the beads and reaction of the immobilized BBSA and streptavidin ( $k_{S,B}$ ). The passive rate of encounter of the SPM beads in solution is inhibited by the hydrodynamic resistance that results from the layer of water between the beads. However, the speed of the encounter can be significantly increased by the use of a magnetic field to force the SPM beads. Thus, the rate of this second reaction in the MBA assay would ideally be limited by  $k_{S,B}$ , which was defined by the rotational diffusion coefficient of the beads and the steric mobility of the immobilized streptavidin and biotin.

The concentration at which the hook effect occurs is central to the design of a useful MBA assay, as shown in **Figure 3**, as it defines the upper limit over which the analyte concentration is proportional to the density of aggregates and also strongly influences the sensitivity of the assay. The hook concentration was determined by the streptavidin binding capacity of a specific density for a specific size of SPM bead (results presented in the *Supplementary Information* section). Curve 1 in **Figure S4** presents the response of an MBA assay in which the streptavidin binding capacity was  $7.5 \times 10^{-8}$  M. The maximum number of aggregates occurred at  $\sim 3 \times 10^{-9}$  M. When the streptavidin binding capacity was decreased to  $8 \times 10^{-9}$  M, as shown in curve 2 in **Figure S4**, the hook concentration decreased to  $\sim 3 \times 10^{-10}$  M. Thus, the maximum number of aggregates was found to form at a BBSA concentration that is close to but less than the streptavidin binding capacity of the beads, i.e.,  $S \approx 0$ . This effect is observed in the shift in the maximum of curves 1 and 2 in **Figure 3**.

The sensitivity of the MBA assay was determined by amount of BBSA bound to the streptavidin beads for a specific reaction time, which is defined by reaction 1 if the aggregation of the beads is highly efficient. Reaction 1 can be treated as quasifirst-order for low concentrations of BBSA if  $k_1 \gg k_{-1}$  for the biotin-streptavidin reaction. Under these conditions it can be shown that the concentration of bound BBSA,  $C_B$ , varies with time ( $t$ ) as

$$C_B = C_{b,o} \left[ 1 - \exp\left(-\frac{t}{\tau}\right) \right], \quad (3)$$

where  $C_{b,o}$  is the initial concentration of BBSA in solution and  $\tau$  is a time constant that defines the rate of reaction of  $B$ . The time constant  $\tau = V / k_1 a C_{S,o}$  is a function of the volume of reaction ( $V$ ), initial concentration of streptavidin on the beads ( $C_{S,o}$ ), and total surface area of the beads ( $a$ ). Thus, for a defined reaction time the extent of reaction, and thus sensitivity of the MBA assay, can be predicted to increase for smaller reaction volumes, higher on-rates, larger surface areas, and higher surface densities of streptavidin. This theoretical analysis is consistent with the observation that the sensitivity of the MBA assay increased with the density of streptavidin bound to the SPM beads, as shown by the apparent increase in sensitivity of curves 1 and 3 in **Figure S4**. This analysis also suggests that the MBA assay sensitivity will decrease at a critical density of the SPM beads, and a significant decrease was observed at bead concentrations below  $10^6$  beads/mL (results not presented).

### Identification of novel anti-HSV peptides

Novel peptide-based binding reagents against purified HSV-1 were identified by screening a bacteriophage library displaying

dodecapeptides and containing approximately one billion independent clones (*Experimental*). **Figure 4A** presents the end-point binding signal, as determined by direct immuno-assay, of the amplified eluted phage pool obtained after each round of selection, using HRP-conjugated anti-pVIII monoclonal antibodies (see *Supporting Information*). The increase in percentage of phage recognizing HSV-1 as biopanning proceeded was reflective of the enrichment of the whole population in favor of displayed peptides specific for HSV-1, and is an indication of the success of the selection procedure.

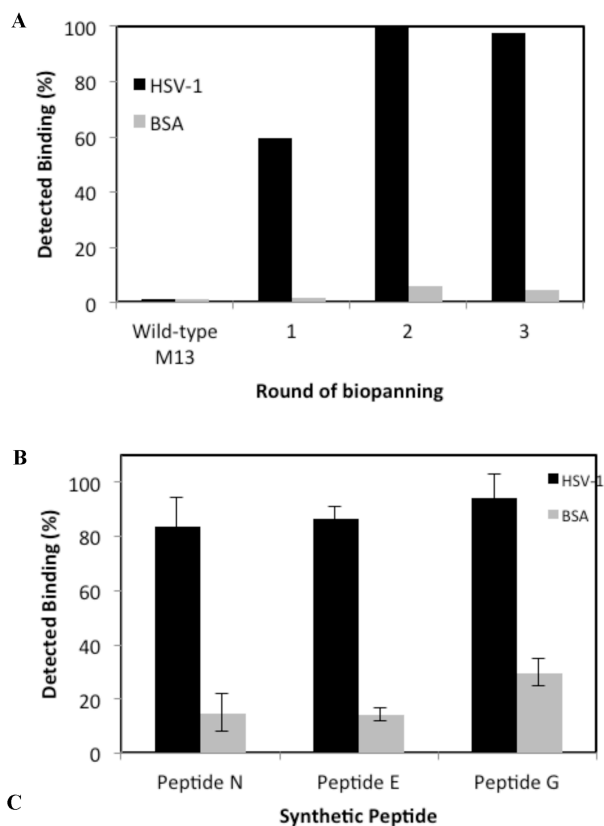


**Figure 4.** Selection of dodecapeptides against HSV-1. **A.** Results of an anti-pVIII immunoassay of whole phage populations after each round of bio-panning. The highest colorimetric intensity was arbitrarily assigned 100% binding and wild-type phage was used as a negative control. **B.** Solid-phase binding of the three synthetic, monovalent peptide constructs to purified HSV-1 virus and BSA. N peptide - NHVHRMHATPAY, E peptide - EHMALTYPFRRP, and G - GPKALSPLMRMG. **C.** Structure of multiple antigenic peptides (MAPs)  $((X_{12})_4K_2KGS\text{GCG})$ , based on a tri-lysine core, permitting peptide branching at the lysine (K)  $\alpha$ - and  $\epsilon$ -amino groups.  $X_{12}$  represents the sequence of amino acids. The spacer (GSGCG) was designed to incorporate a cysteine residue for specific and oriented conjugation to a solid support.

Based on DNA sequencing analysis from the final round phage sequencing, three peptide constructs were designed for synthesis with a C-terminal biotin moiety acting as a reporter for detection in binding experiments. Additionally, a glycine-rich spacer was included in the sequence to mimic the scenario where the peptide is fused to the phage. **Figure 4B** corresponds to the solid phase binding assays using each of the individually synthesized monovalent biotinylated peptides, designated peptides N, E, and G, incubated alongside immobilized HSV-1 and BSA, and followed by extensive washing and detection by streptavidin-HRP. Similar binding intensities for HSV-1 for each of the synthetic peptide structures was observed, and the background on BSA-coated surfaces was uniformly low.

Following confirmation of binding in ELISA assays, a modified, multiple antigenic peptide (MAP) was designed for synthesis, for use in the MBA assay and characterization by surface plasmon resonance (SPR) technology. MAPs offer enhanced binding characteristics over monovalent peptides due to the formation of multiple binding events. The resulting avidity effect is desirable for analyte capture. For conjugation of the MAP to a solid support, a C-terminal single cysteine residue was introduced, which added a unique functional group as there are no other cysteine residue present in the identified sequence. The structure of the final MAP construct used in the MBA assay is provided in **Figure 4C**.

#### C. Detection of HSV-1 using MAP-G functionalized SPMs

MAP-G was used to perform the MBA assay for the detection of HSV-1 by immobilizing biotinylated MAP-G on streptavidin functionalized SPM beads (SPM-G1 beads, *Methods*). The MBA assay was performed with the SPM-G1 beads at a concentration of  $2 \times 10^6$  beads/mL and an incubation time of 30 min. Flow cytometry analysis of the MBA assay was performed for virus concentrations of 2,  $2.1 \times 10^2$ ,  $2.1 \times 10^4$ ,  $2.1 \times 10^6$ , and  $2.1 \times 10^8$  vp/ml, as shown in **Figure S1**, and the distribution of monomers and aggregates is presented in curve 1 in **Figures 5A** and **B**, respectively. These results show that the number of aggregates increased steadily in the presence of HSV-1 at concentrations between 2 and  $2.1 \times 10^6$  vp/ml, and that a hook effect was observed in the HSV-1 response at concentrations greater than  $2.1 \times 10^6$  vp/ml.

The background of HSV-1 SPM-G1 assays significantly influenced the sensitivities of these assays. For BBSA, the aggregates in the blank assays were determined to make-up 8% of the total beads, while for SPM-G1 almost 30% of the monomers aggregated in the absence of HSV-1. This increase in aggregation was attributed to the nonspecific interaction between the MAP-G peptides and the streptavidin on the beads. In order to reduce these nonspecific interactions, streptavidin was eliminated, and a polyethylene glycol (PEG) monolayer was grafted to the surface of the SPM beads, as shown in **Figure 1C**.<sup>26</sup> The PEG monolayer acts to minimize nonspecific interactions and enhanced the steric mobility of the peptide, resulting in a lower background and higher  $k_{S-b}$ . The SPM-G2 and SPM-G3 beads were prepared by covalently grafting the peptides to a monolayer of PEG with BOG-PEG:MPEG ratios of 1:3 and 1:0, respectively. Zeta-potential measurements were performed to characterize each step as a function of pH, as shown in **Figure**

S2, and confirm the inclusion of the PEG monolayer led to a decrease in the surface charge of the beads. The numbers of aggregates in the negative control for SPM-G2 and SPM-G3 decreased to less than 13%. The binding capacity of the SPM-G2 beads for the virus decreased somewhat, but the SPM-G3 construct regained almost full binding capacity with 50% of the beads aggregating at a virus concentration of  $2.1 \times 10^6$  vp/mL. This is consistent with the observation that maximum sensitivities of the MBA assay are achieved for high densities of ligands on the surface of the SPM beads.

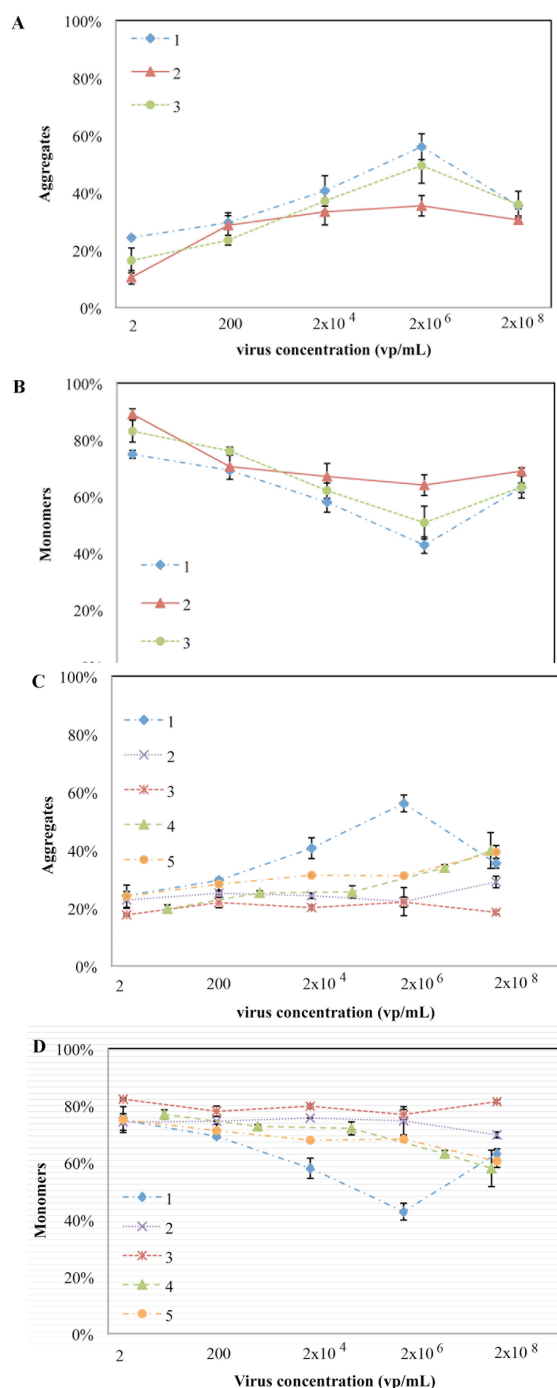


**Figure 5.** HSV MBA assay results for peptide and antibody

functionalized SPM beads. **A.** Aggregates of SPM beads functionalized with peptide G formed as a function of HSV-1 concentration. **1** Aggregates formed through reaction of HSV-1 with SPM-G1 beads, **2** aggregates formed through reaction of HSV-1 with SPM-G2 beads (1:3 ratio of BOC-NH-PEG-NHS:M-PEG-NHS), and **3** aggregates formed through reaction of HSV-1 with SPM-G3 beads (BOC-NH-PEG-NHS coated beads). **B.** Monomers as a function of HSV concentration. The four curves are for the same reactions conditions presented in **A**. **C.** Aggregates of SPM beads functionalized with other peptides and antibodies formed as a function of HSV concentration. **1** HSV-1 assays using SPM-G1 beads, **2** HSV-1 assays using SPM-N beads, **3** HSV-1 assays using SPM-E beads, **4** HSV-2 assays using SPM-G1 beads, and **5** HSV-1 assays using SPM-A beads. **D.** Distribution of monomers as a function of HSV in the aggregation assays described in **C**. In each assay, the concentration of SPMs was  $2 \times 10^6$  beads/mL.

#### Sensitivity of HSV-1 assays using SPM-N and SPM-E beads

The multi-antigenic peptide ligands were further investigated in MBA assays by testing synthetic peptides N and E, which previously demonstrated capacity to detect HSV-1 in ELISA. Immobilization of biotinylated peptides was achieved by simple incubation with streptavidin beads, and curves 2 and 3 in **Figure 5C** present the results of the HSV-1 MBA assay for MAP-N and MAP-E functionalized particles, respectively. Clearly, the formation of aggregates using SPM-N and SPM-E was not significant for virus concentrations over six orders of magnitude. The significant difference in the binding of different peptide ligands to HSV-1 is likely due to the physico-chemical properties of the virus and peptides. In ligand-pathogen interactions, initial attraction is commonly attributed to weak forces, such as, van der Waals and electrostatic charges, enabling the reactants to come into close proximity, before specific interactions begin to dominate and reinforce binding.<sup>27</sup> The large number of glycoprotein spikes on the surface of HSV-1 produces a strong physical barrier, inhibiting the interaction of the virus with micron scale structures such as the SPM beads. Characterization of HSV-1 surface charge by zeta potential analysis suggested the viral particle has a strong negative charge, which is consistent with previous measurements.<sup>28</sup> Peptide G had a positive charge while peptides N and E were less charged. Additionally, it has been reported that immobilization of peptides can significantly reduce peptide activity.<sup>29</sup> To further investigate this phenomenon the binding kinetics of MAP-N and MAP-E to HSV-1 was studied using SPR, and confirmed the inability of HIV-1 to bind to biotinylated peptides immobilized on a streptavidin sensor chip. Taken together, these observations appear to explain the lack of aggregates formed using peptides N and E in the MBA assay.

#### Response of SPM-G1 beads for HSV-2

MBA assays using SPM-G1 beads were also performed with HSV-2 virus to determine if the construct was specific for the HSV-1 strain. The assays were performed at similar conditions to the previously reported HSV-1 assays with SPM bead concentration of  $2 \times 10^6$  beads/ml and HSV-2 at  $1.6 \times 10^3$ ,  $1.6 \times 10^5$ ,  $1.6 \times 10^7$ , and  $1.6 \times 10^9$  vp/ml dilutions. The resulting distribution of aggregates and monomers of SPM-G1 for these HSV-2 assays are

presented in curve 4 of Figure 5C and D, respectively. Clearly, an insignificant growth of aggregates was observed until quite high virus concentrations were reached, i.e.,  $1.6 \times 10^7$  and  $1.6 \times 10^9$  vp/mL. Moreover, the hook effect, observed previously, was not observed for HSV-2. This suggests that the interaction between HSV-2 and MAP-G lacks the specificity necessary to induce significant aggregation. HSV-2, therefore, is not suitable for detection by MAP-G.

### HSV-1 assays using antibody functionalized beads

The viability of commercially available antibodies targeting HSV-1 for use in the MBA assay, was also investigated. A monoclonal antibody was characterized by ELISA and found to be effective in the detection of HSV-1 (*Supplementary Information*). Surface plasmon resonance measurements determine a dissociation constant of  $K_D = 6.33 \times 10^{-8}$  M, which is in the typical range for antibody-antigen interaction. The antibody was immobilized on SPM beads using protein A to enable optimal orientation and maximize interaction with the target. Curve 5 in **Figure 5C** presents the results of the aggregation assays using SPM-A beads at a concentration of  $2 \times 10^6$  beads/mL for HSV-1 concentrations in the range of  $2.1 \times 10^2$  to  $2.1 \times 10^8$  vp/mL. Clearly, a large increase in aggregation was not observed with this antibody-bead construct, although aggregation was observed to increase by 10 percent at a concentration of  $2.1 \times 10^8$  vp/mL of HSV-1. The lack of recognition by anti-HSV antibodies may be a result of the interference of antibody immobilization and/or viral surface glycoproteins on the surface of HSV-1. These results are consistent with the significantly lower on-rate measured for the antibody compared to MAP-G (**Table 1**).

**Table 1.** Reaction kinetics for multi-antigenic peptide G and anti-HSV-1 monoclonal antibody binding to HSV-1. Peptide affinity was measured using steady state binding and antibody affinity was deduced from affinity constants ( $K_D = k_{off}/k_{on}$ ) from multi-cycle kinetics.

	$K_{on}$ ( $M^{-1} s^{-1}$ )	$R_{max}$ (RU)	$K_D$ (M)
MAP-G	$9.6 \times 10^{10}$	189	$1 \times 10^{-11}$
	$K_{on}$ ( $M^{-1} s^{-1}$ )	$K_{off}$ ( $s^{-1}$ )	$K_D$ (M)
Anti-HSV-1 Antibody	$8.1 \times 10^4$	$5.1 \times 10^{-3}$	$6.3 \times 10^{-8}$

### Structural analysis of SPM-G bead complexes with HSV-1

To gain an understanding of the exceptionally high sensitivity of the HSV-1 assay, the interaction of the virus with the SPM-G1 beads was studied with transmission electron microscopy (TEM). Initially, the HSV-1 virion was examined using uranyl acetate negative staining, as shown in Figure 6A and the size of the virus was determined to be between 150 and 200 nm. Structural elements of the virus, such as the envelope, tegument, and capsid, were distinguishable in these studies, and are consistent with the high-resolution cryo-TEM studies of HSV. Figure 6C presents an image of the surface of MAP-G modified SPM beads that were smooth down to the nanometer scale. Figure 6D presents images of SPM-G1 beads after incubation with a high concentration of HSV-1, fixation with glutaraldehyde, and negative staining by uranyl acetate. These images reveal objects on the surface of the beads approximately 30 to 100 nanometer in

size that appear to result from the binding of the virus. Figure 6F presents a high-resolution image of the interface of two SPM beads after incubation with HSV-1 and application of a magnetic field. The material between the beads appears to be consistent with the aggregation of the SPM beads through interaction with HSV-1. These images confirm that the interaction of the virus with the SPM beads occur over a significant area of contact, which is consistent with multivalent binding.

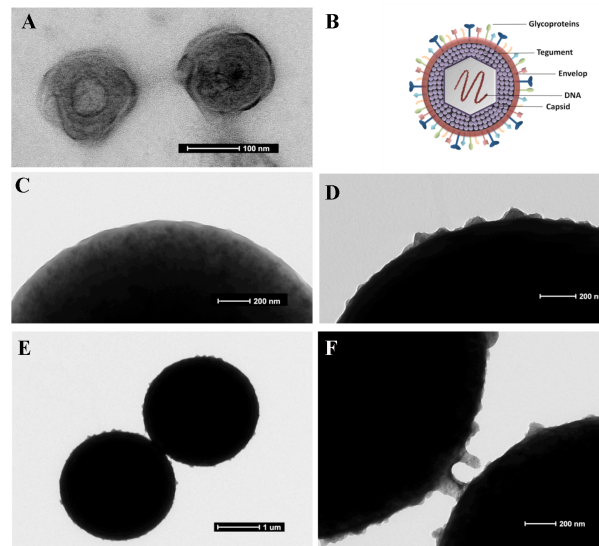


**Figure 6.** Transmission electron microscope study of the HSV-1 and the aggregation of HSV-1 on SPM beads. **A** TEM image of herpes simplex viruses stained with uranyl acetate showing the three layers that are characteristic of these large viruses. **B** Schematic of the structure of HSV virus with capsid, tegument, and envelope. **C** TEM image of the surface of SPM-G1 particles. **D** TEM image of the surface of a SPM-G1 bead after incubated with HSV-1 using negative staining. **E**, **F** TEM images of SPM-G1 particles after incubated with HSV-1 using negative staining.

### Conclusions

This article has demonstrated that the MBA assay is capable of sensitive and rapid detection of proteins and the HSV-1 virus. Highly uniform SPM beads enabled the rapid detection of aggregate sizes, one particle at a time, using light scattering. Biotinylated albumin was detected over six orders of magnitude for reaction times as short as 2 minutes with a sensitivity in the femtomolar range. Analysis of the kinetics of binding indicated that sensitivity of the MBA assay will increase for smaller reaction volumes, higher on-rates, larger surface areas, and higher surface densities of ligand. The MBA assay was also used to detect HSV-1 at concentrations spanning six orders of magnitude. Antibodies against HSV-1 proved to be unsuitable for this MBA assay, and the identification of a novel peptide structure with high affinity for HSV-1 proved crucial to the successful development of the assay. This was attributed to the complex structure of the virus, which is known to contain up to 750 glycoprotein spikes that appear to inhibit the reaction of the virus with the micron size SPM beads. Ultrastructure characterization of the SPM bead

interaction with HSV-1 virus suggests that the mechanism for the increased sensitivity of the virus assay was the multivalent interaction of the virus with the surface of the beads. We also report the successful reduction in monomer aggregation by use of a PEG monolayer. The lowest level of detection was 200 virus particles/mL for reaction times of 30 min. The speed and sensitivity of the MBA assay were linked to the enhanced rates of reaction of an analyte with a suspension of beads and the subsequent use of a magnetic force to collect the SPM beads and accelerate bead aggregation. These results suggest that the MBA assay could prove to be a powerful tool for the detection of viral infections in a point of care setting, with FC having already been implemented in a miniaturized format<sup>30,31</sup>. A limitation of the MBA assay was the decrease in aggregation at high concentrations of analyte that result from the saturation of the SPM bead surfaces, but this can be overcome by careful design of the assay based on the principles described in this article.

## Acknowledgements

This work was funded by the Science Foundation Ireland (08/IN/2972, 08/RP1/B1376, 08/IN.1/B2072 TIDA Feasibility 10, and TIDA 08/IN.1/B2072). We would like to thank Mark Platt, Dr. Gemma Cannon, Dr. David O'Connell, Dr. Alfonso Blanco, and Ms. Tina O'Neill for their helpful discussions regarding this work.

## Notes and references

<sup>a</sup> Conway Institute for Biomolecular and Biomedical Science, and School of Chemistry and Chemical Biology, University College Dublin, Belfield, Dublin 4, Ireland

<sup>b</sup> These authors contributed equally to this publication.

<sup>c</sup> Centre for Research on Infectious Diseases, School of Medicine, University College Dublin, Belfield, Dublin 4, Ireland.

\*Correspondence should be addressed to [gil.lee@ucd.ie](mailto:gil.lee@ucd.ie) Fax: +353

(0)716 1178; Tel: +353 (0) 716 2399

† Electronic Supplementary Information (ESI) available: description of materials, experimental techniques, and discussion of the influence of reaction time, magnetic force, bead size, and binding capacity on the streptavidin-biotin MBA assay. See DOI: 10.1039/b000000x/

1. Chayavichitsilp, P., Buckwalter, J., Krakowski, A. C., and Friendlander, S. F., *Pediatr. Rev.*, 2009, **30**, 119-130.
2. Tyler, K. L., *Herpes*, 2004, **11**, 57A-64A.
3. Koenig, M., Reynolds, K. S., Aldous, W., and Hickman, M., *Diag. Micr. Infect. Dis.*, 2001, **40**, 107-110.
4. Gardella, C., Huang, M.-L., Wald, A., Magaret, A., Selke, S., Morrow, R., and Corey, L., *J. Obstet. Gynecol.*, 2010, **115**, 1209-1216.
5. Slomka, M. J., Emery, L., Munday, P. E., Moulds, M., and Brown, D. W. G., *J. Med. Virol.*, 1998, **55**, 177-183.
6. Verano, L., and Michalski, F. J., *J. Clin. Microbiol.*, 1995, **33**, 1378-1379.
7. Sandhu, A., Handa, H., and Abe, M., *Nanotechnology*, 2010, **21**(44), 442001.
8. Kojima, T., Takei, Y., Ohtsuka, M., Kawarasaki, Y., Yamane, T., and Nakano, H., *Nucleic Acids Res.*, 2005, **33**.
9. Whiteaker, J. R., Zhao, L., Zhang, H. Y., Feng, L.-C., Piening, B. D., Anderson, L., and Paulovich, A. G., *Anal. Biochem.*, 2007, **362**, 44-54.
10. Chang, W. S., Shang, H., Perera, R. M., Lok, S. M., Sedlak, D., Kuhn, R. J., Lee, G. U., *Analyst*, 2008, **133**, 233-240.

11. Beveridge, J. S., Stephens, J. R., Latham, A. H., and Williams, M. E., *Anal. Chem.*, 2009, **81**, 9618-9624.
12. Pamme, N., *Lab Chip*, 2007, **7**, 1644-1659.
13. Pamme, N., and Wilhelm, C., *Lab Chip*, 2006, **6**, 974-980.
14. Afshar, R., Moser, Y., Lehnert, T., and Gijs, M. A. M., *Anal. Chem.*, 2011, **83**, 1022-1029.
15. Park, S. Y., Ko, P. J., Handa, H., and Sandhu, A., *J. Appl. Phys.*, 2010, **107**.
16. Baudry, J., Rouzeau, C., Goubault, C., Robic, C., Cohen-Tannoudji, L.; Koenig, A., Bertrand, E., and Bibette, J., *Proc. NATL. ACAD. U.S.A.*, 2006, **103**, 16076-16078.
17. Koh, I., Hong, R., Weissleder, R., and Josephson, L., *Anal. Chem.*, 2009, **81**, 3618-3622.
18. Grünewald, K., Desai, P., Winkler, D. C., Heymann, J. B., Belnap, D. M., Baumeister, W., and Steven, A. C., *Science*, 2003, **302**, 1396-1398.
19. Gomara, M. J., Riedemann, S., Vega, I., Ibarra, H., Ercilla, G., and Haro, I., *J. Immunol. Methods*, 2000, **234**, 23-34.
20. Greijer, A. E., van de Crommert, J. M. G., Stevens, S. J. C., and Middeldorp, J. M., *J. Clin. Microbiol.*, 1999, **37**, 179-188.
21. Li, Z., Bai, X. F., and Bian, H. J., *Clin. Chem.*, 2002, **48**, 645-647.
22. Olson, G. L., Bolin, D. R., Bonner, M. P., Bos, M., Cook, C. M., Fry, D. C., Graves, B. J., Hatada, M., Hill, D. E., Kahn, M., Madison, V. S.; Rusiecki, V. K., Sarabu, R., Sepinwall, J., Vincent, G. P., and Voss, M. E., *J. Med. Chem.*, 1993, **36**, 3039-3049.
23. Yahi, N., Sabatier, J. M., Baghdiguian, S., Gonzalezscarano, F., Fantini, J., *J. Virol.*, 1995, **69**, 320-325.
24. Fassina, G., Corti, A., Cassani, G., *Int. J. Pept. Protein Res.*, 1992, **39**, 549-556.
25. Fassina, G.; Cassani, G.; Corti, A., *Arch. Biochem. Biophys.*, 1992, **296**, 137-143.
26. Lee, G. U.; Metzger, S.; Natesan, M.; Yanavich, C.; Dufrene, Y. F., *Anal. Biochem.*, 2000, **287**, 261-271.
27. Costa, F.; Carvalho, I. F.; Montelaro, R. C.; Gomes, P.; Martins, M. C. L., *Acta Biomater.*, 2011, **7**, 1431-1440.
28. Karlin, S.; Brendel, V., *Proc. Natl. Acad. Sci. U.S.A.*, 1988, **85**, 9396-9400.
29. Bagheri, M., Beyermann, M., and Dathe, M., *Antimicrob. Agents Chemother.*, 2009, **53**, 1132-1141.
30. Li, P., Kilinc, D., Ran, Y.-F and G.U Lee., *Lab Chip*, 2013, **13**, 4400-4408.
31. Platt, M., Willmott, G.R. and G.U Lee, *Small*, 2012, **8**, 2436-2444.
32. Fields, C., Mallee, P., Muzard, J and Lee, G. U., *Food Chemistry*, 2012, **134**, 1831-1838.